

## Observing the Quantum Wave Nature of Free Electrons through Spontaneous Emission

Roei Remez,<sup>1,\*</sup> Aviv Karnieli,<sup>1,\*</sup> Sivan Trajtenberg-Mills,<sup>1</sup> Niv Shapira,<sup>1</sup> Ido Kaminer,<sup>2</sup> Yossi Lereah,<sup>1</sup> and Ady Arie<sup>1</sup>

<sup>1</sup>*School of Electrical Engineering, Fleischman Faculty of Engineering, Tel Aviv University, Tel Aviv 69978, Israel*

<sup>2</sup>*Department of Electrical Engineering, Technion–Israel Institute of Technology, Haifa 32000, Israel*

 (Received 29 October 2018; revised manuscript received 3 April 2019; published 6 August 2019)

We investigate, both experimentally and theoretically, the interpretation of the free-electron wave function using spontaneous emission. We use a transversely wide single-electron wave function to describe the spatial extent of transverse coherence of an electron beam in a standard transmission electron microscope. When the electron beam passes next to a metallic grating, spontaneous Smith-Purcell radiation is emitted. We then examine the effect of the electron wave function transversal size on the emitted radiation. Two interpretations widely used in the literature are considered: (1) radiation by a continuous current density attributed to the quantum probability current, equivalent to the spreading of the electron charge continuously over space; and (2) interpreting the square modulus of the wave function as a probability distribution of finding a point particle at a certain location, wherein the electron charge is always localized in space. We discuss how these two interpretations give contradictory predictions for the radiation pattern in our experiment, comparing the emission from narrow and wide wave functions with respect to the emitted radiation's wavelength. Matching our experiment with a new quantum-electrodynamics derivation, we conclude that the measurements can be explained by the probability distribution approach wherein the electron interacts with the grating as a classical point charge. Our findings clarify the transition between the classical and quantum regimes and shed light on the mechanisms that take part in general light-matter interactions.

DOI: [10.1103/PhysRevLett.123.060401](https://doi.org/10.1103/PhysRevLett.123.060401)

Spontaneous radiation from charged particles has long been a major field of interest for many quantum electrodynamical (QED) investigations. A large group of such phenomena, with implications on both fundamental science and technology, is the radiation from free electrons: Cherenkov [1], transition [2], diffraction [3], undulator [4], and Smith-Purcell [5] radiation are common examples. Although these effects can be almost fully explained by a classical theory of radiation excited by the motion of point charges, the wave nature of the particles can only be accounted for by a fully quantum theory, namely QED.

Attempts to incorporate the notion of the electron wave function into our classical understanding of radiation through Maxwell's equations could be done in different ways and introduce subtle ambiguities. Interestingly, this problem dates to the very first days of quantum mechanics. The interpretation of the square modulus of the electron wave function  $|\psi|^2$  multiplied by the electron charge  $e$  and velocity  $\mathbf{v}$  as the current density, was contemplated by Erwin Schrödinger, leading to a theoretical inconsistency regarding the interaction with the electromagnetic field [6]. This mystery was resolved by Born [7], by interpreting the wave function as the probability amplitude. Nevertheless, the interpretation of the wave function still gives rise to different approaches in the literature even today, with certain problems treating the charge and current densities of a single electron as the source of radiation [8–11], or

disregarding the consequences of considering a wide electron beam [12–15]. These approaches, while theoretically appealing, contradict our understanding of spontaneous emission as an incoherent process emerging from quantized charged particles. Therefore, our aim is to revisit the fundamental question of the interpretation of the wave function by investigating Smith-Purcell radiation as a representative of spontaneous radiation phenomena from free electrons. Our findings point to conclusions that might also be relevant for a variety of related light-electron quantum effects.

Smith-Purcell radiation (SPR) has been the subject of intense investigation since its discovery in 1953 [5]. The radiation, generated by the passage of a swift electron next to a grating, has the potential of creating light sources in wavelength ranges which are unreachable using other technologies, such as deep UV and x ray [16,17]. Many classical theories, treating the electron as a *point charge*, were developed to explain this phenomenon. These include constructive interference [5], derivation of the reflected fields due to the electron evanescent field [18], as well as analyzing the induced currents on the grating's surface [19]. On the other end of the theoretical spectrum, QED analysis treated the electron as a *plane wave* in the transverse dimension [20–26], explained in quantum terms the Smith-Purcell dispersion relation [20,21], predicted quantum corrections [22], and analyzed the effect of the

longitudinal size of the single electron on stimulated [24] and spontaneous [26] radiation. The radiation pattern in the point-particle limit of classical physics and the plane-wave solution of QED in the zero-recoil limit agree as a consequence of the correspondence principle, as  $\hbar$  is absent in both results. In this regime, the radiation is always spatially diverging [see Fig. 1(a)].

However, when trying to describe wide but finite electron beams, one may encounter difficulties reconciling the classical and quantum theories for the following reasons. First, electron optical elements, used to shape and focus electron beams in electron microscopy, coherently manipulate the phase of the electron wave function [27,28]. Second, currents not exceeding 50 nA ensure that on average, only a single electron impinges on a sample, if the interaction length with the latter is short ( $\leq 100 \mu\text{m}$ ) and the electron is swift ( $v > 0.1c$ , where  $c$  is the speed of light). Last, under quite standard working conditions it is possible to generate electron beams with very large transverse coherence (significantly larger than optical wavelengths) using field emission guns (FEGs) [29–32]. Following the former arguments, this large coherence of electron beams can be attributed to the width of a single-electron wave function. This observation renders the semiclassical treatment ambiguous, as will be described below.

To describe radiation from wide electron beams semiclassically, a few approaches were employed: classical, transverse line currents were used to model the beam, predicting the interaction with two dimensional  $c$ -shaped arrays [12], two dimensional hole arrays [13,14], and two dimensional photonic crystals [23]. Another example is the Maxwell-Schrödinger approach [11,33], wherein the Schrödinger wave function of the electron is solved, and the current density is derived from it, thereby acting as a source term in Maxwell's equations.

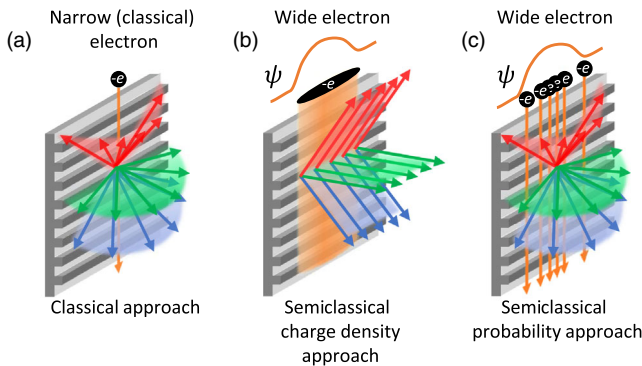


FIG. 1. Schematic description of the research question. (a) A classical point charge electron produces highly diverged radiation. (b) The charge-density semi classical approach predicts collimated radiation. (c) The probability semiclassical approach predicts high divergence as in the classical treatment.

In these methods, the emitted radiation is calculated classically, and the spatial coherence of the source current is an underlying assumption. This is equivalent to saying that the electron charge is distributed in space according to the squared amplitude of the wave function. Let us consider for simplicity that an electron beam has been coherently focused to a wave packet state  $\psi(\mathbf{r}, t) = \psi_T(\mathbf{r}_T, z - vt) \exp[ikz - i(E/\hbar)t]$  [ $E$ ,  $k$ , and  $v$ , are the electron's energy, wave vector and group velocity, respectively, and  $\mathbf{r}_T = (x, y)$ ]. Let us assume that the slowly varying transverse wave packet  $|\psi_T|^2$  has only a lateral width  $d$  parallel to the rulings of the grating [ $x$  axis in Fig. 1(b)]. Following Reimer and Kohl [27], we identify the electron current as  $\mathbf{J} = e(\hbar/2m_e i)\psi\nabla\psi + c.c. \cong e\mathbf{v}|\psi_T|^2$  (where  $\mathbf{v} = \hat{\mathbf{z}}\hbar k/m_e$  with  $m_e$  denoting the electron mass) resulting in the line currents employed in Refs. [20–24]. Following Jackson [34], we obtain a classical relation between the spectral radiant power of the wide current density and the point-particle result:

$$\left(\frac{d^2 P}{d\Omega d\omega}\right)_{\text{line}} = \left| \int dx |\psi_T(x)|^2 e^{-i\hat{\mathbf{n}} \cdot \hat{\mathbf{x}} qx} \right|^2 \left(\frac{d^2 P}{d\Omega d\omega}\right)_{\text{point}} \quad (\text{incorrect}), \quad (1)$$

where  $q = 2\pi/\lambda$  is the wave number of the emitted radiation of wavelength  $\lambda$ , and  $\hat{\mathbf{n}}$  is the direction of observation. If the wave function's transverse range much exceeds the radiated wavelength, i.e.,  $d \gg \lambda$ , then the Fourier transform prefactor in the above equation becomes a sharp distribution in  $\hat{\mathbf{n}} \cdot \hat{\mathbf{x}}$ , centered around 0 and having a width  $\sim \lambda/d$ . Therefore, Maxwell's equations predict that this radiation should be collimated in the ruling's direction ( $\hat{\mathbf{n}} \cdot \hat{\mathbf{x}} = 0$ ), with reduced azimuthal divergence, as illustrated in Fig. 1(b).

However, an alternative semiclassical approach can give contradictory conclusions [see Fig. 1(c)]: the electron always interacts with the grating as a point charge, and the transverse shape of  $|\psi|^2$  gives the probability density for the transverse coordinate of the interaction. According to this treatment, which is used, for example, in electron energy loss spectroscopy [35] and in photon-induced near-field electron microscopy [36,37], the correct input to Maxwell's equations in a semiclassical treatment is a moving point charge, located randomly in the transverse coordinate according to a probability distribution  $|\psi|^2$ :  $(d^2 P/d\Omega d\omega)_{\text{line}} = \int dx |\psi_T(x)|^2 (d^2 P/d\Omega d\omega)_{\text{point}}$  [see also Eq. (4)]. The emitted radiation in this case will not be collimated, no matter what the lateral width of  $|\psi_T|^2$  is, since the radiation is emitted from a point each time (and is averaged over different points according to the transverse width of the wave function).

In the following, we investigate SPR from a wide electron beam both experimentally and theoretically. In the single-electron-at-a-time regime, our experimental and theoretical results show that for different wave packet widths the emitted radiation is always highly diverged in the azimuthal dimension, with no significant difference in the angular distribution, pointing towards the probability distribution approach as the correct interpretation of the wave function.

The experimental setup is presented in Fig. 2. A metallic grating of period 416 nm was placed inside the viewing chamber of a 200 keV FEI Tecnai transmission electron microscope (TEM). The lenses of the TEM were used to manipulate the electron beam spatial profile. The experiment was repeated twice: for a narrow and a wide electron beam. As we show below, both experiments resulted in the same angular distribution.

FEG TEMs usually demonstrate very large transverse coherence lengths (TCLs). In our case, the TCL of the beam was estimated by the Fresnel fringe method [27,38] at the limiting aperture of 150  $\mu\text{m}$  in diameter. The method, limited mainly by the SNR of the TEM image, provides a lower bound on the coherence length, measured to be 2.5  $\mu\text{m}$  [Fig. (S2) in the Supplemental Material [39]]. In order to obtain large SNR in the emitted radiation, we used

a high current density. However, the TCL can be much larger if lower current densities and smaller apertures are used, wherein TCL values exceeding one millimeter were reported using a biprism [30,31], and holograms of tens of microns in size were successfully used to generate desired patterns in the far field [47–49]. It is well known that the ratio between the transverse coherence length and the beam size is conserved in electron optical systems [29,31,32]; therefore, measuring the beam waist on any other plane of the optical system provides a lower bound estimate for the coherence length.

The beam was first corrected for astigmatism and focused to the smallest spot possible. This narrow beam, 300  $\mu\text{m}$  in size, has a TCL of at least 5  $\mu\text{m}$ , according to the considerations employed above. The wide beam was generated, using the same electron source, by adjusting the stigmator lens so that the focus of the ruling axis alone was obtained closer to the lens. As a result, the beam size at the grating location was increased to 2000  $\mu\text{m}$ , giving a TCL of at least 33  $\mu\text{m}$ , more than 60 times larger than the optical wavelength. As in most Smith-Purcell experiments, all electrons eventually hit the grating, and the interaction length (estimated to be  $\sim 10 \mu\text{m}$ ) is determined by the angle between the electron beam and the grating [50]. Comparing the interaction length to the average spacing between electrons in the beam,  $d_{\text{avg}} = 800 \mu\text{m}$  (for a current of 40.8 nA), shows that our experiment is done at the single-electron regime.

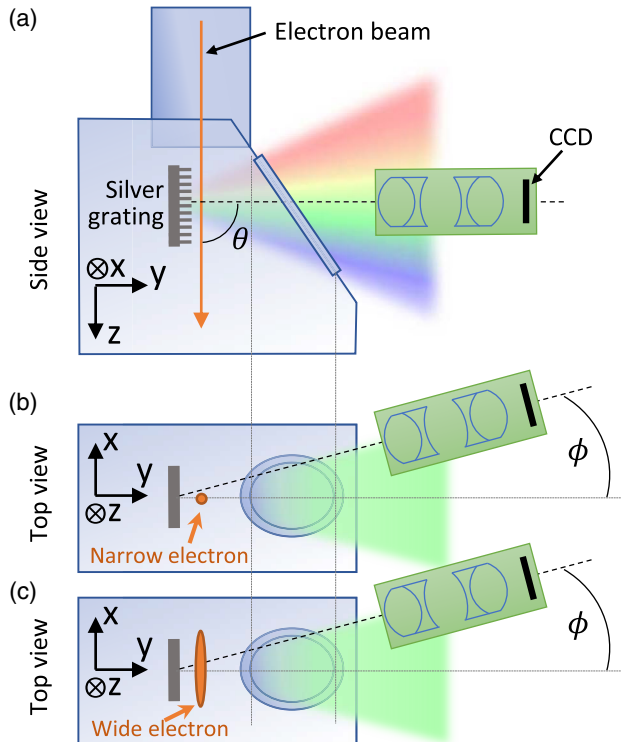


FIG. 2. Experimental setup. (a) Side view of the viewing chamber of the transmission electron microscope. (b) and (c) top view of the setup for the case of a narrow (b) and wide (c) electron beam. The radiated power was measured in both cases for different values of  $\phi$ .

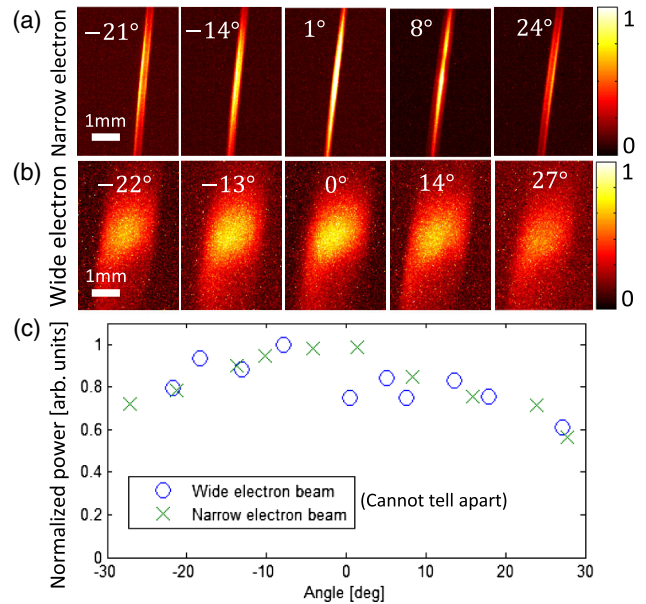


FIG. 3. Experimental results. (a) and (b) images of the grating plane as observed for the case of narrow and wide electron beams, respectively, for different values of the azimuthal angle  $\phi$  (marked). (c) Normalized power of SPR as a function of the azimuthal angle  $\phi$  for narrow and wide electron beams, showing no significant difference between the two. The split in the measured stripe in (a) at wide angles is a result of double reflection from the viewing chamber window.

In order to measure the Smith-Purcell radiation, two achromatic doublets were positioned outside the viewing chamber of the TEM, imaging the grating plane on a CCD camera. Let us define  $\theta$ , the elevation angle, as the angle between the photon momentum and the  $z$  axis, whereas  $\phi$ , the azimuthal angle, is the angle between the projection of the photon momentum on the  $xy$  plane and the  $y$  axis, where the axes are defined in Fig. 2. Figures 3(a) and 3(b) present the images acquired for angle  $\theta = \pi/2$ , for different  $\phi$  values and for narrow (a) and wide (b) electron beams. As can be seen in Fig. 3(c), the difference in angular spread between the beams is not significant, and that in both cases the spatial divergence is large, decreasing to about 60% at around 30 deg. Were the current density interpretation of the wave function true, there should have been a significant difference in the divergence between the two experiments, proportional to the ratio between the TCLs of the two beams (differing by almost an order of magnitude). More specifically, the wide beam should have resulted in a divergence of  $(\lambda/d) \approx 15$  mrad, or 0.87 deg, which is about 30 times

smaller than the measured value of 30 deg. Therefore, it is evident that only the probabilistic point charge analysis of the phenomenon agrees with the experiment.

The theoretical analysis of the spontaneous emission pattern of *arbitrarily wide* Dirac electrons passing above a periodic grating is detailed below. The initially noninteracting system of photons and a single electron is subject to the unperturbed Dirac Hamiltonian,

$$H_0 = c\boldsymbol{\alpha} \cdot \mathbf{p} + \beta m_e c^2 + \sum_{\mathbf{q}, n\sigma} \hbar\omega_{\mathbf{q}n\sigma} a_{\mathbf{q}n\sigma}^\dagger a_{\mathbf{q}n\sigma}, \quad (2)$$

where  $\boldsymbol{\alpha} = (\alpha_1, \alpha_2, \alpha_3)$  and  $\beta$  are the Dirac matrices,  $\mathbf{p} = -i\hbar\nabla$  the momentum operator for the electron,  $\omega_{\mathbf{q}n\sigma}$ ,  $a_{\mathbf{q}n\sigma}$  the frequency and annihilation operator of the electromagnetic field,  $\mathbf{q}$  the photon momentum,  $\sigma = 1, 2$  the two polarizations, and  $n$  the band index of the periodic modes. The boundary conditions due to the periodic grating (of period  $\Lambda$ ) along the  $z$  axis impose periodic modes for the electromagnetic field:

$$\mathbf{A} = \sum_{\mathbf{q}, n, \sigma} \sqrt{\frac{\hbar}{2\epsilon_0 V \omega_{\mathbf{q}, n, \sigma}}} \left( a_{\mathbf{q}, n, \sigma} \sum_{m=-\infty}^{\infty} \boldsymbol{\epsilon}_{m, \mathbf{q}n\sigma}(\mathbf{r}_T) A_{m, \mathbf{q}n\sigma}(\mathbf{r}_T) e^{i\mathbf{q}_m \cdot \mathbf{r}} + \text{H.c.} \right), \quad (3)$$

where  $\epsilon_0$  is the vacuum permittivity, and  $V$  the quantization volume. Each mode  $\mathbf{q}\sigma n$  is composed of an infinite number of momenta components with index  $m$  and momentum  $\mathbf{q}_m = \mathbf{q} + (0, 0, \kappa_m) = (q_x, q_y, q_z + \kappa_m)$ , where  $\kappa_m = m(2\pi/\Lambda)$  and  $q_{ym} = \sqrt{|\mathbf{q}|^2 - (q_z + \kappa_m)^2 - q_x^2}$  (thus giving  $\mathbf{q}_{m=0} = \mathbf{q}$ ), and  $\boldsymbol{\epsilon}_{m, \mathbf{q}\sigma n}$  is the field polarization vector of the  $m$ th component (a unit vector in space). The  $A_{m, \mathbf{q}\sigma n}$  coefficients satisfy a normalization condition over the transverse coordinate  $\mathbf{r}_T = (x, y)$   $\sum_m \int d^2\mathbf{r}_T |A_{m, \mathbf{q}\sigma n}|^2 = 1$  (the mode normalization is approximated by the regular free-space form, as we shall later restrict ourselves to free-space dispersion).

The modes  $\mathbf{q}\sigma n$  corresponding to SPR resonances have a propagating part  $e^{i\mathbf{q}_0 \cdot \mathbf{r}}$  and evanescent parts for  $m > 0$  [21]. Only the evanescent part of the mode carries enough longitudinal momentum,  $q_z + \kappa_m$ , necessary for momentum conservation in the Smith-Purcell emission. When an SPR photon is detected in the far field, its generation was made possible due to the interaction of the electron with the *evanescent* part (near field) of the same mode it occupied (see Fig. 4).

The interaction Hamiltonian is readily given by taking  $\mathbf{p} \rightarrow \mathbf{p} + e\mathbf{A}$  in the Dirac Hamiltonian in Eq. (2), i.e.,  $H_{\text{int}} = eca \cdot \mathbf{A}$ . The transition rate for spontaneous emission  $w_{\mathbf{q}, n\sigma}^{sp}$  between the initial and final states can be calculated using the Fermi golden rule [21]. For this manner, we describe the initial electron-photon state as a superposition of free-space electron modes

multiplied by the electromagnetic vacuum  $|\psi_i\rangle = |0\rangle \otimes \sum_{\mathbf{k}_i} \mathbf{u}_i(\mathbf{s}_i, \mathbf{k}_i) (1/\sqrt{V}) \tilde{\psi}(\mathbf{k}_i) |\mathbf{k}_i\rangle$ , where  $\mathbf{u}_i$  is the initial four-component spinor of the electron (with spin state  $\mathbf{s}_i$ ), and where  $\tilde{\psi}(\mathbf{k}_i)$  is the initial spectral envelope of the wave function, assumed to be sharply peaked near the carrier initial wave vector  $\mathbf{k}_{0i}$ . This assumption means that the electron wave function has a slowly varying envelope (SVE) in the spatial domain [51]. The spectral radiant power  $P$  per unit solid angle  $\Omega$  per frequency  $\omega$  is  $(d^2P/d\Omega d\omega) = \hbar\omega \sum_{n, \sigma} \rho_{\text{ph}}(\omega, \mathbf{q}n\sigma) w_{\mathbf{q}n\sigma}^{sp}$ , where  $\rho_{\text{ph}}$  is the photon density of states. If  $\rho_{\text{ph}}$  and  $\omega_{\mathbf{q}n\sigma}$

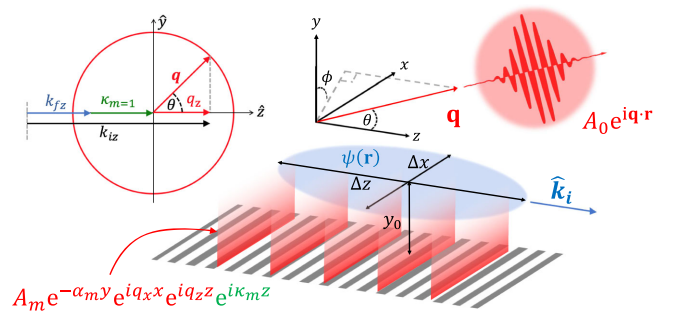


FIG. 4. Illustration of spontaneous Smith-Purcell emission from a wide electron. Left, momentum space description for  $\phi = 0$ . Right, real space. The blue cloud above the grating represents the electron wave function that interacts with the periodic evanescent electromagnetic field (red), thanks to the additional momentum provided by the grating (green).

approximated by their free-space expressions,  $V\omega^2/2\pi^3c^3$ , and  $cq$ , respectively, and when the zero-recoil limit for the electron (valid for  $\hbar\omega \ll 2m_e c^2\gamma$ ) is assumed, we find (full derivation is available in section C of the Supplemental Material [39])

$$\frac{d^2P}{d\Omega d\omega} = \int d^2\mathbf{r}_T |\psi_T(\mathbf{r}_T)|^2 \frac{d^2P^{\text{class}}}{d\Omega d\omega}(\mathbf{r}_T), \quad (4)$$

where  $\psi_T(\mathbf{r}_T)$  is the transverse part of the spatial electron wave function. In Eq. (4),  $(d^2P^{\text{class}}/d\Omega d\omega)(\mathbf{r}_T)$  denotes the ‘‘classical’’ radiation pattern for a point particle at the transverse position  $\mathbf{r}_T$ :

$$\begin{aligned} \frac{d^2P^{\text{class}}}{d\Omega d\omega}(\mathbf{r}_T) &= \frac{\hbar c^2 \alpha \beta}{(\beta^{-1} - \cos\theta)^3} \sum_{n\sigma} \sum_{m=-\infty}^{\infty} \kappa_m^2 |\mathcal{E}_{m,\mathbf{q}n\sigma}(\mathbf{r}_T)|^2 \\ &\times \frac{\text{sinc}^2\left[\frac{\omega - \omega_{\text{SP},m}}{\Delta\omega_{\text{int}}}\right]}{\pi \Delta\omega_{\text{int}}}, \end{aligned} \quad (5)$$

where  $\alpha = e^2/4\pi\epsilon_0\hbar c$  is the fine structure constant and  $\beta = v/c$  is the dimensionless electron velocity. In the above expression, we defined the evanescent mode transverse envelope as  $|\mathcal{E}_{m,\mathbf{q}n\sigma}(\mathbf{r}_T)|^2 = e^{-2\alpha_m y} |\hat{\mathbf{z}} \cdot \hat{\mathbf{e}}_{m,\mathbf{q}n\sigma}^* A_{m,\mathbf{q}n\sigma}^*(\mathbf{r}_T)|^2$ , containing the familiar exponential decay away from the grating plane (note that  $\alpha_m = -iq_{ym} > 0$  is the evanescent wave inverse decay length). The radiation pattern consists of a series of resonances centered about the classical (zero order in  $\hbar$ ) SP frequencies  $\omega_{\text{SP},m} = c\kappa_m/(\beta^{-1} - \cos\theta)$ . Each resonance is broadened due to the finite interaction length of the electron  $L_{\text{int}}$ , thereby introducing the interaction bandwidth  $\Delta\omega_{\text{int}} = [c/(\beta^{-1} - \cos\theta)](2/L_{\text{int}})$ .

Remarkably, we can interpret Eq. (4) by considering semiclassical arguments. Indeed, it appears that the correct semiclassical interpretation is the one described in Fig. 1(c). The emission from a ‘‘classical’’ electron, Eq. (5) and Fig. 1(a), depends on the location of that electron within the evanescent mode. When the more accurate treatment of a quantum electron with an arbitrarily wide wave function is employed, it introduces a transverse probability density  $p(\mathbf{r}_T) = |\psi_T(\mathbf{r}_T)|^2$ , and the emitted radiation is the weighted average over all point-particle emissions along the transverse dimension. This is equivalent to saying that the wide quantum electron is emitting radiation like a classical point electron, thereby emitting azimuthally divergent radiation, with some probability determining where the interaction would occur precisely.

Our experimental results, backed with the theoretical derivation, show that the azimuthal dependence of the emitted radiation does not change with the width of the beam. In other words, the continuous current density interpretation of the wave function is refuted. The results imply that the theoretical analysis of some previous works rely on an incorrect description of electron beams. In contrast, our theory suggests an interesting and nontrivial

semiclassical interpretation to the emission process, implying that the Smith-Purcell effect from slowly varying, nonrecoiled electron wave packets is local even in the quantum regime. This interpretation might shed light on the mechanisms that take part within the process of spontaneous emission from free electrons, such as electron wave function decoherence, or collapse [52], and perhaps also clarify the transition between the classical and quantum regimes of such problems. Moreover, the probability density description of the wide electron should be valid to other radiation mechanisms from wide electrons, such as optical diffraction radiation [53], and presumably also to other charged negative and positive particles, including muons, protons, and positrons.

An interesting outlook from this study is to extend the quantum analysis to the regime of temporally coherent, wide multiple-electron pulses [54,55]. In the classical description, photons that are emitted from different electrons in the same electron pulse can interfere, and the spatial coherence of the beam affects the radiation pattern [34,56]. In the quantum picture, a single paraxial electron wave packet can never demonstrate this phenomenon. This follows from our study, as well as other arguments such as charge quantization (the single electron cannot be divided into smaller constituents that may radiate coherently). However, it is not forbidden that a multiparticle state of copropagating electrons emits photons that coherently interfere, as predicted by the classical analysis [56]. The emitted optical angular spectrum might, therefore, provide a clear distinction between electron beams that carry a single electron or multiple electrons.

We thank Professor Avi Gover and Dr. Yiming Pan for stimulating discussions, and Dr. George Levi for his assistance in the electron coherence measurements. The work was supported by DIP, the German-Israeli Project cooperation, by the Israel Science Foundation, Grant No. 1415/17. A.K. is supported by the Adams Fellowship Program of the Israel Academy of Science and Humanities. S.T.-M. is supported by the Ministry of Science Shulamit Aloni scholarship.

\*These authors contributed equally.

†Corresponding author.

roei.remez@gmail.com

- [1] P. A. Cherenkov, Visible emission of clean liquids by action of gamma radiation, *Dokl. Akad. Nauk SSSR* **2**, 451 (1934).
- [2] I. M. Frank and V. L. Ginzburg, Radiation of a uniform moving electron due to its transition from one medium into another, *Zh. Eksp. Teor. Fiz.* **16**, 15 (1946) [*J. Phys. USSR* **9**, 353 (1945)].
- [3] Y. N. Dnestrovskii and D. P. Kostomarov, Radiation from a modulated beam of charged particles when passing through a circular hole in a plane screen, *Dokl. Akad. Nauk SSSR* **124** (1959).

- [4] H. Motz, W. Thon, and R. N. Whitehurst, Experiments on radiation by fast electron beams, *J. Appl. Phys.* **24**, 826 (1953).
- [5] S. J. Smith and E. M. Purcell, Visible light from localized surface charges moving across a grating, *Phys. Rev.* **92**, 1069 (1953).
- [6] R. P. Feynman, R. B. Leighton, and M. L. Sands, *The Feynman Lectures on Physics* Vol. III, (Basic Books, New York, 2011).
- [7] M. Born, Born's Nobel lecture on the statistical interpretation of quantum mechanics, Nobel Lecture Technical Report, 1954, <https://www.nobelprize.org/prizes/physics/1954/born/facts/>.
- [8] M. Lewenstein, P. Balcou, M. Y. Ivanov, A. L'Huillier, and P. B. Corkum, Theory of high-harmonic generation by low-frequency laser fields, *Phys. Rev. A* **49**, 2117 (1994).
- [9] W. Becker, A. Lohr, M. Kleber, and M. Lewenstein, A unified theory of high-harmonic generation: Application to polarization properties of the harmonics, *Phys. Rev. A* **56**, 645 (1997).
- [10] E. Lorin, S. Chelkowski, and A. Bandrauk, A numerical Maxwell-Schrödinger model for intense laser-matter interaction and propagation, *Comput. Phys. Commun.* **177**, 908 (2007).
- [11] N. Talebi, Schrödinger electrons interacting with optical gratings: Quantum mechanical study of the inverse Smith-Purcell effect, *New J. Phys.* **18**, 123006 (2016).
- [12] Z. Wang, K. Yao, M. Chen, H. Chen, and Y. Liu, Manipulating Smith-Purcell Emission with Babinet Meta-surfaces, *Phys. Rev. Lett.* **117**, 157401 (2016).
- [13] L. Liang, W. Liu, Y. Liu, Q. Jia, L. Wang, and Y. Lu, Multicolor and multidirectional-steerable Smith-Purcell radiation from 2D sub-wavelength hole arrays, *Appl. Phys. Lett.* **113**, 013501 (2018).
- [14] S. Liu, M. Hu, Y. Zhang, Y. Li, and R. Zhong, Electromagnetic diffraction radiation of a subwavelength-hole array excited by an electron beam, *Phys. Rev. E* **80**, 036602 (2009).
- [15] C. Luo, M. Ibanescu, S. G. Johnson, and J. D. Joannopoulos, Cerenkov radiation in photonic crystals, *Science* **299**, 368 (2003).
- [16] S. E. Korbly, A. S. Kesar, J. R. Sirigiri, and R. J. Temkin, Observation of Frequency-Locked Coherent Terahertz Smith-Purcell Radiation, *Phys. Rev. Lett.* **94**, 054803 (2005).
- [17] M. J. Moran, X-Ray Generation by the Smith-Purcell Effect, *Phys. Rev. Lett.* **69**, 2523 (1992).
- [18] P. M. van den Berg, Smith-Purcell radiation from a point charge moving parallel to a reflection grating, *J. Opt. Soc. Am.* **63**, 1588 (1973).
- [19] J. H. Brownell, J. Walsh, and G. Doucas, Spontaneous Smith-Purcell radiation described through induced surface currents, *Phys. Rev. E* **57**, 1075 (1998).
- [20] S. J. Glass and H. Mendlowitz, Quantum theory of the Smith-Purcell experiment, *Phys. Rev.* **174**, 57 (1968).
- [21] A. Friedman, A. Gover, G. Kurizki, S. Ruschin, and A. Yariv, Spontaneous and stimulated emission from quasifree electrons, *Rev. Mod. Phys.* **60**, 471 (1988).
- [22] S. Tsesses, G. Bartal, and I. Kaminer, Light generation via quantum interaction of electrons with periodic nanostructures, *Phys. Rev. A* **95**, 013832 (2017).
- [23] H. Fares and M. Yamada, A quantum mechanical analysis of Smith-Purcell free-electron lasers, *Nucl. Instrum. Methods Phys. Res., Sect. A* **785**, 143 (2015).
- [24] A. Gover and Y. Pan, Dimension-dependent stimulated radiative interaction of a single electron quantum wavepacket, *Phys. Lett. A* **382**, 1550 (2018).
- [25] H. Fares and M. Yamada, A quantum mechanical analysis of Smith-Purcell free-electron lasers, *Nucl. Instrum. Methods Phys. Res., Sect. A* **785**, 143 (2015).
- [26] Y. Pan and A. Gover, Spontaneous and stimulated emissions of a preformed quantum free-electron wave function, *Phys. Rev. A* **99**, 052107 (2019).
- [27] L. Reimer and H. Kohl, *Transmission Electron Microscopy: Physics of Image Formation* (Springer, New York, 2008).
- [28] H. Lichte and M. Lehmann, Electron holography—Basics and applications, *Rep. Prog. Phys.* **71**, 016102 (2008).
- [29] T. Latychevskaia, Spatial coherence of electron beams from field emitters and its effect on the resolution of imaged objects, *Ultramicroscopy* **175**, 121 (2017).
- [30] B. Cho and C. Oshima, Electron beam coherency determined from interferograms of carbon nanotubes, *Bull. Korean Chem. Soc.* **34**, 892 (2013).
- [31] B. Cho, T. Ichimura, R. Shimizu, and C. Oshima, Quantitative Evaluation of Spatial Coherence of the Electron Beam from Low Temperature Field Emitters, *Phys. Rev. Lett.* **92**, 246103 (2004).
- [32] G. Pozzi, Theoretical considerations on the spatial coherence in field emission electron microscope, *Optik (Stuttg.)* **77**, 69 (1987).
- [33] N. Talebi, Interaction of electron beams with optical nanostructures and metamaterials: From coherent photon sources towards shaping the wave function, *J. Opt.* **19**, 103001 (2017).
- [34] J. D. Jackson, *Classical Electrodynamics* (Wiley, New York, 1999).
- [35] R. H. Ritchie and A. Howie, Inelastic scattering probabilities in scanning transmission electron microscopy, *Philos. Mag.* **A 58**, 753 (1988).
- [36] B. Barwick, D. J. Flannigan, and A. H. Zewail, Photon-induced near-field electron microscopy, *Nature (London)* **462**, 902 (2009).
- [37] S. T. Park, M. Lin, and A. H. Zewail, Photon-induced near-field electron microscopy (PINEM): Theoretical and experimental, *New J. Phys.* **12**, 123028 (2010).
- [38] J. C. H. Spence, W. Qian, and M. P. Silverman, Electron source brightness and degeneracy from Fresnel fringes in field emission point projection microscopy, *J. Vac. Sci. Technol. A* **12**, 542 (1994).
- [39] See Supplemental Material at <http://link.aps.org/supplemental/10.1103/PhysRevLett.123.060401> for experimental details, coherence measurement, the detailed QED derivation and analysis of the dispersion relation under the zero-recoil and SVE approximations, which also includes Refs. [40–46].
- [40] C. Murdia, N. Rivera, T. Christensen, L. J. Wong, J. D. Joannopoulos, M. Soljačić, and I. Kaminer, Controlling

- light emission with electron wave interference, [arXiv: 1712.04529](#).
- [41] C. Kremers, D.N. Chigrin, and J. Kroha, Theory of Cherenkov radiation in periodic dielectric media: Emission spectrum, *Phys. Rev. A* **79**, 013829 (2009).
- [42] M.E. Peskin and D.V. Schroeder, *An Introduction To Quantum Field Theory* (Westview Press, Reading, 1995).
- [43] J.D. Joannopoulos, S.G. Johnson, J.N. Winn, and R.D. Meade, *Photonic Crystals: Molding the Flow of Light*, 2nd ed. (Princeton University Press, Princeton, 2008).
- [44] C. W. Hsu, B. Zhen, A. D. Stone, J. D. Joannopoulos, and M. Soljačić, Bound states in the continuum, *Nat. Rev. Mater.* **1**, 16048 (2016).
- [45] B. Zhen, C. W. Hsu, Y. Igarashi, L. Lu, I. Kaminer, A. Pick, S.-L. Chua, J. D. Joannopoulos, and M. Soljačić, Spawning rings of exceptional points out of Dirac cones, *Nature (London)* **525**, 354 (2015).
- [46] C. W. Hsu, B. Zhen, J. Lee, S.-L. Chua, S. G. Johnson, J. D. Joannopoulos, and M. Soljačić, Observation of trapped light within the radiation continuum, *Nature (London)* **499**, 188 (2013).
- [47] R. Shiloh, Y. Lereah, Y. Lilach, and A. Arie, Sculpturing the electron wave function using nanoscale phase masks, *Ultramicroscopy* **144**, 26 (2014).
- [48] R. Shiloh, Y. Tsur, R. Remez, Y. Lereah, B. A. Malomed, V. Shvedov, C. Hnatovsky, W. Krolikowski, and A. Arie, Unveiling the Orbital Angular Momentum and Acceleration of Electron Beams, *Phys. Rev. Lett.* **114**, 096102 (2015).
- [49] N. Voloch-Bloch, Y. Lereah, Y. Lilach, A. Gover, and A. Arie, Generation of electron Airy beams, *Nature (London)* **494**, 331 (2013).
- [50] R. Remez, N. Shapira, C. Roques-Carnes, R. Tirole, Y. Yang, Y. Lereah, M. Soljačić, I. Kaminer, and A. Arie, Spectral and spatial shaping of Smith-Purcell radiation, *Phys. Rev. A* **96**, 061801(R) (2017).
- [51] Conveniently, since the electron momentum is typically larger by 5–6 orders of magnitude with respect to the photon momentum, there still exists a relatively wide regime where the SVE approximation holds, even when the wave function momentum spread  $\Delta k$  is larger than the photon momentum.
- [52] Q. Fu, Spontaneous radiation of free electrons in a non-relativistic collapse model, *Phys. Rev. A* **56**, 1806 (1997).
- [53] P. Karataev, S. Araki, R. Hamatsu, H. Hayano, T. Muto, G. Naumenko, A. Potylitsyn, N. Terunuma, and J. Urakawa, Beam-Size Measurement with Optical Diffraction Radiation at KEK Accelerator Test Facility, *Phys. Rev. Lett.* **93**, 244802 (2004).
- [54] M. Krüger, M. Schenk, and P. Hommelhoff, Attosecond control of electrons emitted from a nanoscale metal tip, *Nature (London)* **475**, 78 (2011).
- [55] P. Hommelhoff, Y. Sortais, A. Aghajani-Talesh, and M. A. Kasevich, Field Emission Tip as a Nanometer Source of Free Electron Femtosecond Pulses, *Phys. Rev. Lett.* **96**, 077401 (2006).
- [56] C. J. Hirschmugl, M. Sagurton, and G. P. Williams, Multi-particle coherence calculations for synchrotron-radiation emission, *Phys. Rev. A* **44**, 1316 (1991).